SMEI 3D Reconstruction of a Coronal Mass Ejection Interacting with a Corotating Solar Wind Density Enhancement: The 2008 April 26 CME

Jackson, B. V.; Buffington, A.; Hick, P. P.; Clover, J. M.; Bisi, M. M.; Webb, D. F.

Published in:
Astrophysical Journal

DOI:
10.1088/0004-637X/724/2/829

Publication date:
2010

Citation for published version (APA):
Jackson, B. V., Buffington, A., Hick, P. P., Clover, J. M., Bisi, M. M., & Webb, D. F. (2010). SMEI 3D Reconstruction of a Coronal Mass Ejection Interacting with a Corotating Solar Wind Density Enhancement: The 2008 April 26 CME. *Astrophysical Journal*, *724*(2), 829-834. https://doi.org/10.1088/0004-637X/724/2/829

The Astrophysical Journal, 724:829–834, 2010 December 1 doi:10.1088/0004-637X/724/2/829

SMEI 3D RECONSTRUCTION OF A CORONAL MASS EJECTION INTERACTING WITH A COROTATING SOLAR WIND DENSITY ENHANCEMENT: THE 2008 APRIL 26 CME

B. V. Jackson[1], A. Buffington[1], P. P. Hick[1,2], J. M. Clover[1], M. M. Bisi[1,3], and D. F. Webb[4]
[1] Center for Astrophysics and Space Sciences, University of California at San Diego, 9500 Gilman Drive, #0424, La Jolla, CA 92093-0424, USA
[2] San Diego Supercomputer Center, University of California at San Diego, 9500 Gilman Drive #0505, La Jolla, CA 92093-0505, USA
[3] Institute of Mathematics and Physics, Aberystwyth University, Penglais Campus, Aberystwyth, SY23 3BZ Wales, UK
[4] Institute for Space Research, Boston College, Chestnut Hill, MA, 02467, USA
Received 2010 June 18; accepted 2010 September 16; published 2010 November 9

ABSTRACT

The Solar Mass Ejection Imager (SMEI) has recorded the brightness responses of hundreds of interplanetary coronal mass ejections (CMEs) in the interplanetary medium. Using a three-dimensional (3D) reconstruction technique that derives its perspective views from outward-flowing solar wind, analysis of SMEI data has revealed the shapes, extents, and masses of CMEs. Here, for the first time, and using SMEI data, we report on the 3D reconstruction of a CME that intersects a corotating region marked by a curved density enhancement in the ecliptic. Both the CME and the corotating region are reconstructed and demonstrate that the CME disrupts the otherwise regular density pattern of the corotating material. Most of the dense CME material passes north of the ecliptic and east of the Sun–Earth line: thus, in situ measurements in the ecliptic near Earth and at the *Solar-TErrestrial RElations Observatory Behind* spacecraft show the CME as a minor density increase in the solar wind. The mass of the dense portion of the CME is consistent with that measured by the Large Angle Spectrometric Coronagraph on board the *Solar and Heliospheric Observatory* spacecraft, and is comparable to the masses of many other three-dimensionally reconstructed solar wind features at 1 AU observed in SMEI 3D reconstructions.

Key words: solar–terrestrial relations – solar wind – Sun: coronal mass ejections (CMEs) – Sun: heliosphere – Sun: rotation

1. INTRODUCTION

Coronal mass ejections (CMEs) as observed by a coronagraph and their interplanetary counterparts measured near 1 AU have masses that are often approximately the same, but occasionally very different (e.g., Jackson et al. 2006, 2008a; Bisi et al. 2010). While there are many CME observations in the heliosphere, and in situ measurements of their interplanetary counterparts (ICMEs), because of the large distances and potential interactions, it is often uncertain what changes occur as an event propagates outward from the Sun to where it is observed near 1 AU (Zhang et al. 2007). This article concentrates on the 2008 April 26 CME event that was observed first in coronagraph white-light imagery, and later by the Solar Mass Ejection Imager (SMEI; Eyles et al. 2003; Jackson et al. 2004), and in situ by plasma monitors on the *Solar-TErrestrial RElations Observatory Behind (STEREO-B)* spacecraft (Kaiser et al. 2008). In this article, we use the term "CME" for the coronagraph-observed eruption as well as its SMEI-observed counterpart in the interplanetary medium.

SMEI was launched in 2003 January on the Air Force Space Test Program satellite Coriolis. Precisely, calibrated SMEI images and the long-term (>2 week) removal of background contaminant light (stars and the zodiacal light) are required for optimum display of typical slow- and fast-moving heliospheric structures in sky maps, and especially for their three-dimensional (3D) reconstruction. Further, processing removes contaminant lunar brightness and high-energy particle hits present in the SMEI images as the instrument passes through the South Atlantic Anomaly (SAA) and the auroral ovals. In this same procedure, brightness from the aurora (Mizuno et al. 2005) is also removed from the SMEI data at sidereal locations selected to be devoid of bright stars (Jackson et al. 2008a). The time-dependent reconstruction algorithm (Jackson et al. 2001, 2002, 2006, 2008b, and references therein) allows us to isolate both the CME and the corotating enhanced density structure from surrounding heliospheric material, and determine their masses and 3D extent. These reconstructions are also re-imaged at an enhanced brightness contrast relative to the direct images, but at somewhat reduced spatial and temporal resolutions in order to discern the angular extents and general shape of the associated heliospheric structures and to map their outward progress from the Sun.

Section 2 briefly describes the 2008 April 26–29 CME observations. Section 3 presents the results of the analyses: the location, volume, and mass of dense material within the CME, its relationship to the corotating density structure, and comparison of the 3D reconstruction with in situ measurements. We conclude in Section 4.

2. OBSERVATIONS

The *Solar and Heliospheric Observatory* (*SOHO*; Domingo et al. 1995)—Large Angle and Spectroscopic COronagraph (LASCO) C2 (inner coronagraph) instrument (Brueckner et al. 1995) first detected a partial-halo CME in Thomson-scattered white light difference images on 2008 April 26 at 14:30 UT. This followed surface activity including a *GOES* 10 B3.8 level X-ray event and a coronal wave, dimming and arcade formation observed in the *SOHO* Extreme-ultraviolet Imaging Telescope (EIT; Delaboudiniere et al. 1995) beginning about an hour earlier at approximately 13:30 UT. The plane-of-the-sky velocity for the CME was measured between 515 and 621 km s^{-1} according to the Coordinated Data Analysis Workshops (CDAW) CME catalog: http://cdaw.gsfc.nasa.gov/CME_list. The mass of the CME listed in the CDAW catalog is 3.4×10^{15} g. We also note that this plane-of-the-sky mass estimate has a quality index label "poor." The main CME feature's position angle was 65° with an estimated angular width of the

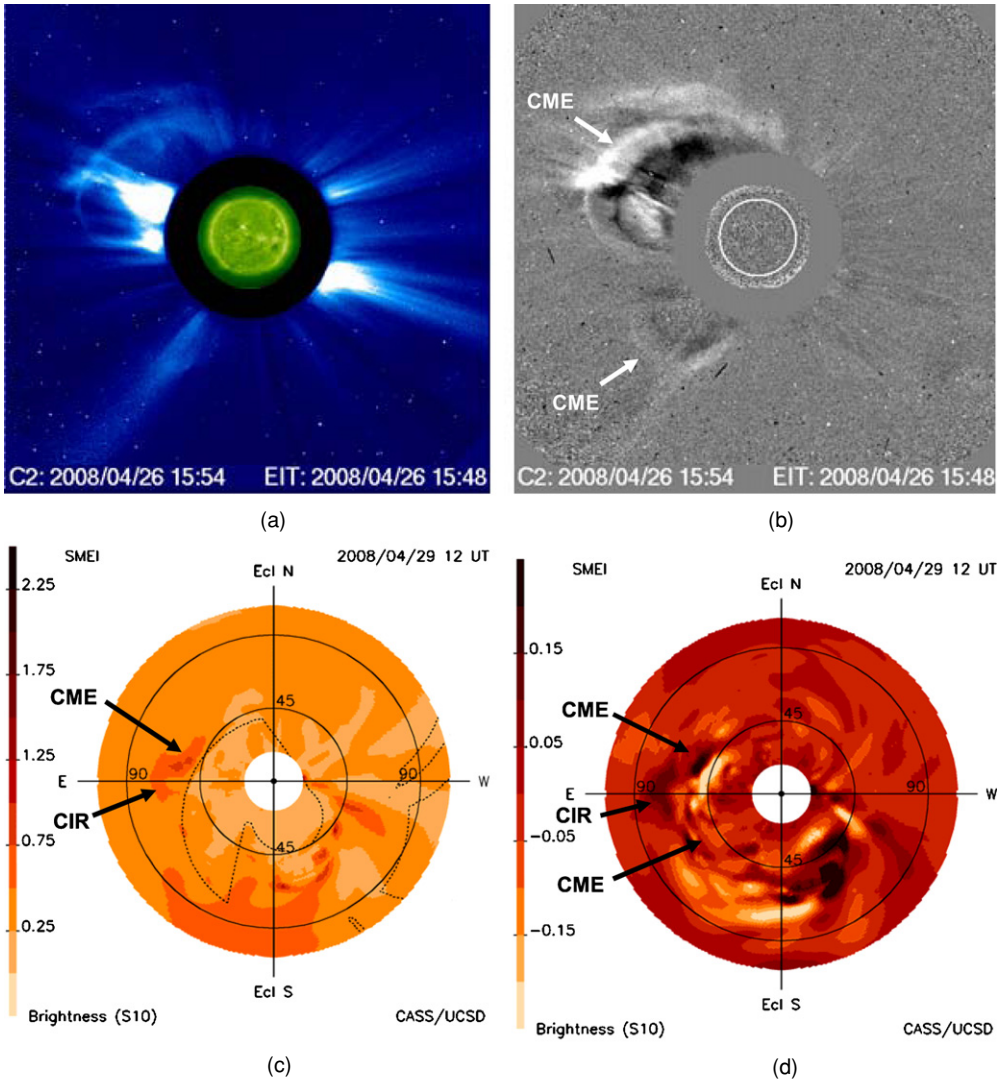

Figure 1. LASCO coronagraph images and SMEI three-dimensionally reconstructed images of the 2008 April 26 CME at the times indicated. In the SMEI views from Earth to an elongation of 110° an r^{-2} density falloff normalized to 1 AU has been removed from the three-dimensionally reconstructed volumes to present both the direct and difference images in calibrated brightness (see scale to the left of each). (a) Direct LASCO C2 coronagraph image with a superimposed 195 Å EIT image. A remnant of the flaring region associated with the CME can just be discerned to the northeast of disk center in EIT. (b) C2 difference image with a superimposed 195 Å EIT difference image. (c) SMEI direct Sun-centered reconstructed image. The dashed lines indicate the regions not viewed in the SMEI cameras at this time, even though the 3D reconstruction has filled them in. This includes a region to an elongation of about 50° east of the Sun along the ecliptic. (d) SMEI Sun-centered difference image.

CME of 281°. Figure 1 shows examples of direct (Figure 1(a)) and difference images (Figure 1(b)) from LASCO C2 on 2008 April 26 at 16:30 UT. The analysis from SMEI, in which a long-term base has been removed, shows the CME when it reached *STEREO-B* about 3 days later (Figure 1(c)). Both the CME and the brightness associated with the corotating structure are shown here, with the CME front better isolated from the corotating structure in the SMEI difference image where the volumetric data from 12 hr earlier has been subtracted (Figure 1(d)). In the present case, difference images show some structure similar to the direct ones, but tend to highlight regions with high brightness gradients in front of the bulk of the CME material (and see Jackson et al. 2009). This analysis shows that the bulk of the dense material associated with the CME event has moved outward to the solar northeast, as shown earlier in coronagraph images. However, some manifestation of the CME also appears to the southeast in the SMEI volumetric differences as is also shown in the coronagraph difference images. The material in the ecliptic is a combination of the CME mass and corotating structure near 1 AU (see Section 3).

3. 3D RECONSTRUCTION RESULTS

This CME event has been analyzed by Odstrcil et al. (2010), using ENLIL and a "cone model" CME approximation (Michałek et al. 2003), and by using an empirical fit to difference images from the twin *STEREO* spacecraft Heliospheric Imagers (HIs; Eyles et al. 2009). The difference images from *STEREO* are modeled in three dimensions by Thernisien et al. (2009) with a croissant flux rope model and by Wood and Howard (2009) using a self-similar approximation to track the approximate location, position, and outward motion of the CME. The SMEI analysis, unlike those using CME modeling alone, reconstructs both the CME and corotating structure total brightness in the

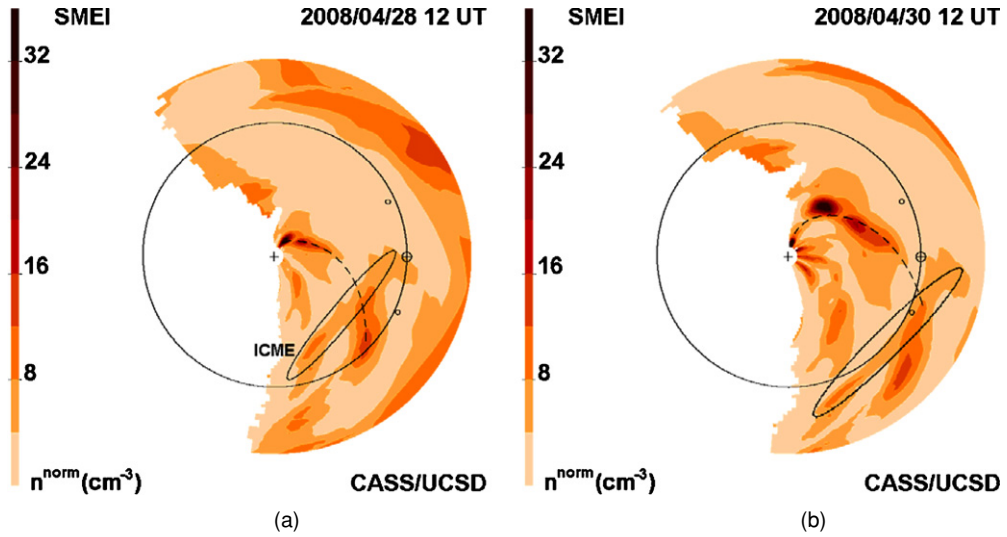

Figure 2. SMEI three-dimensionally reconstructed ecliptic cuts viewed from the north just prior to and following the arrival of the 2008 April 26 CME and corotating density structure at *STEREO-B* (at the dates and times indicated). The Sun is at the center of each plot with the Earth "⊕" shown to the right on its elliptical orbit. Projected locations of both *STEREO-A* and *STEREO-B* are shown ahead of and behind Earth's orbital path, respectively as small circles. In order to view structures at the same density contour level with solar distance, an r^{-2} density falloff normalized at 1 AU has been removed from the volumetric data whose scale is shown to the left of each image. Areas to the left of each cut are left blank since these locations are not accessed in SMEI images, and thus cannot be reconstructed in the ecliptic. The ecliptic location of the CME is indicated by an elongated ellipse and the corotating structure by a dashed line.

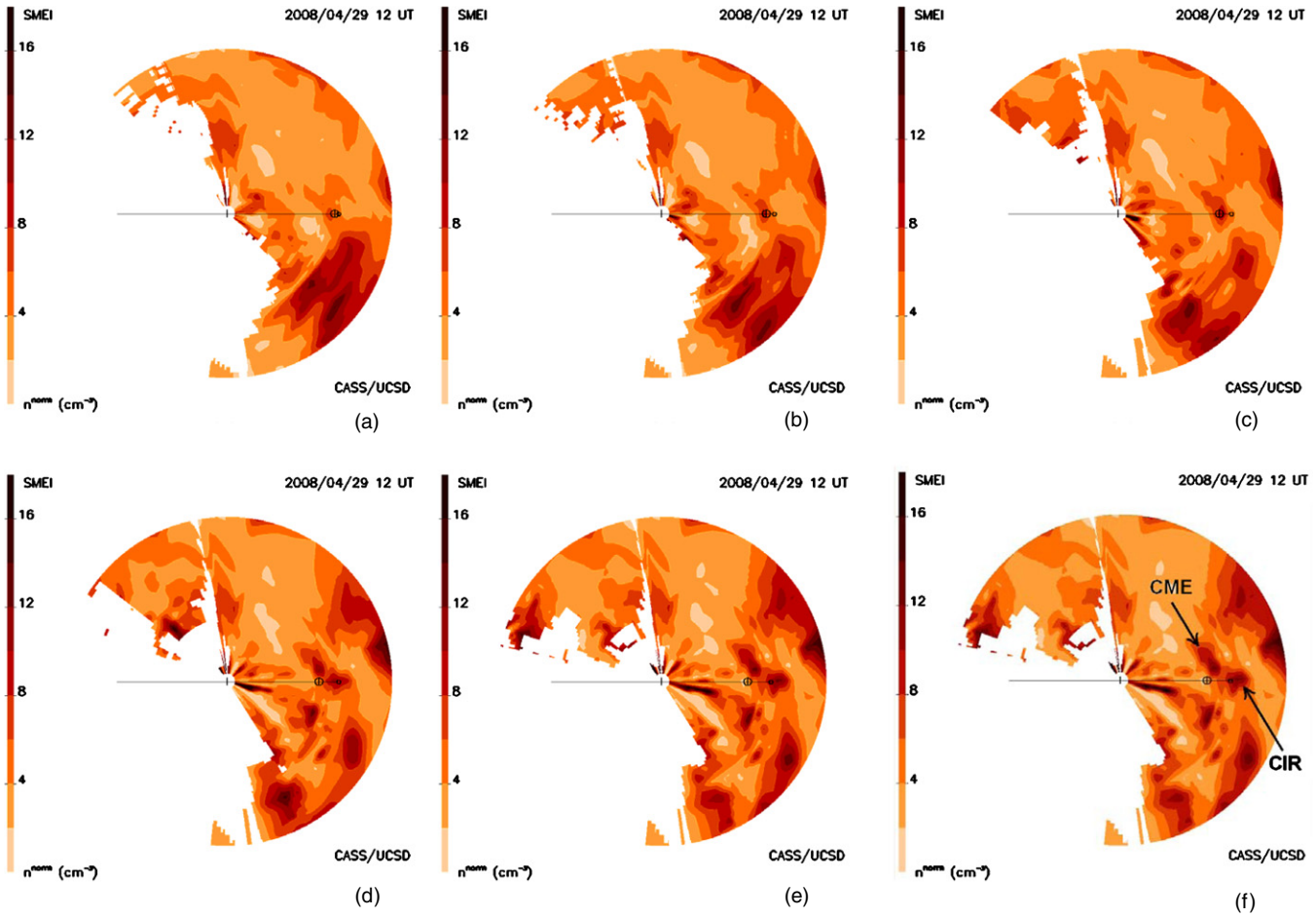

Figure 3. SMEI three-dimensionally reconstructed meridional cuts viewed from the east of Earth at the time of the arrival of the 2008 April 26 CME and corotating density structure at *STEREO-B* at 12 UT on 2008 April 29. The Sun is at the center of each plot with the Earth "⊕" shown to the right on its elliptical orbit (here depicted as a straight line). The projected location of *STEREO-B* is shown on the images as the small circle more distant from the Sun than the Earth. In order to view structures at the same density contour level with solar distance, an r^{-2} density falloff normalized at 1 AU has been removed from the volumetric data whose scale is shown to the left of each image. Areas to the left of each cut are left blank since these locations are not accessed in SMEI images, and thus cannot be reconstructed in the meridional cut. The meridional cuts (a)–(f) are separated by 5° beginning 14° east of the Sun–Earth line; (c) is the meridian that includes *STEREO-B*. The CME and corotating structure "CIR" are labeled in (f).

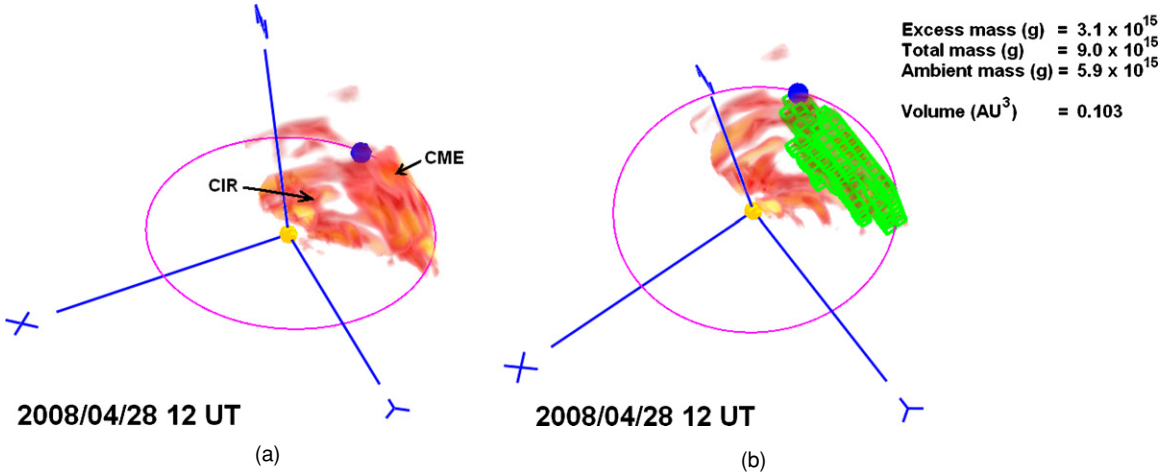

Figure 4. SMEI 3D reconstructions of the 2008 April 26–29 CME and corotating structure density as a remote observer would view it 3 AU from the Sun from the north and east of the Sun–Earth line 12 UT on 2008 April 28. The Sun is in the center of each plot with the Earth above and to the right on its elliptical orbit. An r^{-2} density falloff normalized to 1 AU has been removed from the volumetric data. (a) The dense portion of the CME (labeled) is observed just below and to the right of the Earth in this projection. The ecliptic corotating structure (as shown in Figure 2(a)) is labeled "CIR." (b) The dense CME structure is highlighted by cubes (green) above a 4 N_P cm^{-3} contour level that isolates this density from that of the corotating structure to the south. A cut at the negative vernal equinox direction $X = -0.85$ has been imposed to isolate the CME and eliminate summing the mass from the dense corotating material more distant from the Sun (see Figure 2(a)).

interplanetary medium. It also accommodates their potentially different material outward flows, and in the present instance obtains data to the east of the Sun after the material has reached solar elongations greater than about 50°. The Odstrcil et al. (2010) ENLIL modeling derived from magnetograms of photospheric magnetic field that includes a cone model CME approximation derived from coronagraph images provides information about both corotating and CME structures from near-Sun observations that are altered to best match the in situ results. The SMEI 3D reconstruction analysis, on the other hand, provides information on the combination of both the CME and the corotating structure, but does so entirely from remotely sensed data around the Earth.

Figure 2 is a slice in the ecliptic through the 3D reconstruction at times bracketing the arrival of the CME and corotating dense structure at *STEREO-B*, which at this time was located ∼24° east of the Sun–Earth line. In Figure 2(a), the CME and corotating structure have nearly reached the *STEREO-B* spacecraft, while in Figure 2(b), both the CME and the dense structure associated with the corotating material have passed the spacecraft. In Figure 2(b), the dense corotating structure has reformed, and continues to emanate from the Sun somewhat farther to the west. This material is not continuous, and is broken by the CME as well as having a segmented appearance at several places in the ecliptic to the west of the Sun–Earth line (in particular at about 0.5 AU in Figure 2(b) at 30° west of the Sun–Earth line). The Archimedean spiral curvature of the corotating structure rotates over ∼80° from the Sun to 1 AU, which, since this indicates an outward motion that takes approximately six days to arrive at Earth, implies an outward ecliptic speed of this dense structure ensemble of ∼280 km s^{-1}. This slow speed of the density ensemble marking this corotating region is typical of these same features measured by the Helios spacecraft white-light photometers (Jackson 1991). At *STEREO-B*, the dip in speed at the onset of the density enhancement nearly reaches this low value. While this structure is typical of many observed in Helios photometer data (and more recently in SMEI ecliptic observations), we cannot be certain that it is formed by the interaction of high speed solar wind following slow (a corotating interaction region or CIR). For lack of a better term, we have, however, labeled this feature a "CIR" to distinguish it from the CME in figure annotations. The CME density in the ecliptic is a rather minor feature that appears in front of a region of less dense corotating material that takes about three days to travel from the Sun to Earth. In the analyses shown in Figures 2 and 3 we depict proton density. As in Jackson et al. (2008a), this associates the electron Thomson-scattered brightness with a solar wind density assuming a 10% helium abundance, and thus 20% more electrons than proton density alone would indicate. This enables a more direct comparison of SMEI 3D reconstructions with proton density measured in situ, and permits analysis in terms of N_P.

The bulk of the dense material associated with the CME passes to the north of the ecliptic as shown in Figure 1. This is illustrated in more detail in Figure 3, which shows a sequence of meridional-plane cuts having 5° increments of angular distance from Earth beginning 14° east of the Sun–Earth line. The third image of the sequence (Figure 3(c)) is the meridional cut that includes the *STEREO-B* spacecraft that is located 24° east of the Sun–Earth line at this time. The main portion of the CME is located north of the ecliptic plane with its greatest extent and mass east of *STEREO-B*, where the CME and the corotating structure are also more separated spatially. These results are, by the way, in line with those of Wood and Howard (2009) that show that the CME centered more to the east of *STEREO-B*, that also coincides more with model 1 described in the Lugaz et al. (2010) analysis of this event. This is somewhat different from the analyses of Thernisien et al. (2009) and Odstrcil et al. (2010) that indicate the center of the CME is directed more closely toward the Earth. Figure 4 shows a 3D perspective view of this dense material and that of the corotating structure as a remote observer would see it from the north and east of the Sun–Earth line. The structure reconstructed in the positive *X*-direction in these images has been removed in order to isolate the CME and corotating structure on the hemisphere of the Sun toward the Earth. Figures 3 and 4 also show considerable dense material not associated with the features highlighted in the ecliptic close to Earth but to the east and south of the Sun–Earth line at this time. Figure 4(b) shows the CME material highlighted by cubes (as in Wang et al. 2003; Jackson et al. 2006, 2008a) above a

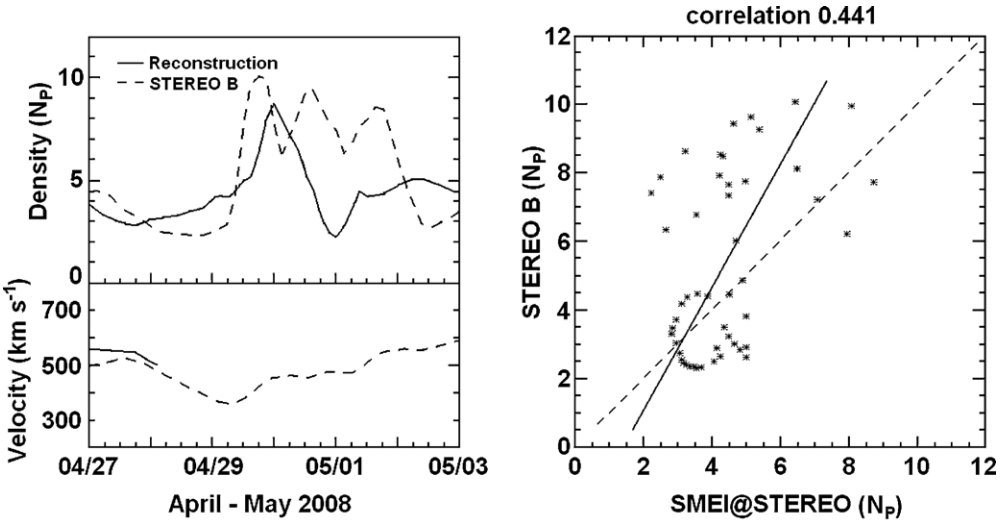

Figure 5. (a) Density and velocity measurements at *STEREO-B* in late April to early 2008 May. (b) Density correlation indicating the variation in the comparison between the in situ measurements and the 3D reconstructions.

4 N_P cm^{-3} contour level. This analysis shows that the CME extends over a volume of at least 0.1 AU^3 and contains at least 3 $\times$ 10^{15} g of excess mass that reached normalized 1 AU densities slightly above 16 N_P cm^{-3} at 12 UT on 2008 October 29 in the center of the CME. A larger percentage (two-thirds) of the CME mass (ambient mass as indicated in Figure 4(b)) is encompassed within the volume defined by the excess mass above the 4 N_P cm^{-3} contour level (see Jackson et al. 2006, 2008a for analyses where the ambient mass comprises only a small fraction of the total). The total mass of the CME within this volume is 9.0 $\times$ 10^{15} g. Interplanetary scintillation (IPS; e.g., Hewish et al. 1964) velocity determinations are incomplete for this time interval, and do not allow good measurement of the 3D velocities or the energy associated with these structures (as they have in some previous analyses; see, e.g., Jackson et al. 2008a).

Figure 5 presents the density derived from the 3D reconstruction at the location of the *STEREO-B* spacecraft, together with in situ density and velocity from the *STEREO-B* PLAsma and SupraThermal Ion Composition (PLASTIC) instrument (Galvin et al. 2008) from 2008 April 27–May 3. The in situ measurements have been averaged using a half-day "boxcar" filter to match the SMEI reconstruction spatial and temporal resolution. Figure 5(b) shows the correlation between reconstructed and in situ density. The overall correlation shows that the onset time of the event's density enhancement was accurately determined above the appropriate base level by the SMEI 3D reconstructions. The velocity, too, was accurately determined at the beginning of the interval where these measurements were available to provide a reconstruction. Following the density-enhancement onset, the measurements from *STEREO-B* show continuing variations in the in situ density at the level of ~8 protons cm^{-3} for a couple of days, but that this is not observed in the 3D reconstruction results. We note that the qualitative 3D modeling reconstructions from Odstrcil et al. (2010) (Figure 6), like those from SMEI, show a decrease in the modeled MHD density response following this CME at the longitude of *STEREO-B* behind the faster CME "Void." We expect that the decrease is most likely a real effect following the event, and that the in situ measurements at *STEREO* relate to local density variations that are not well resolved by either the 3D reconstructions or the MHD response shown by ENLIL.

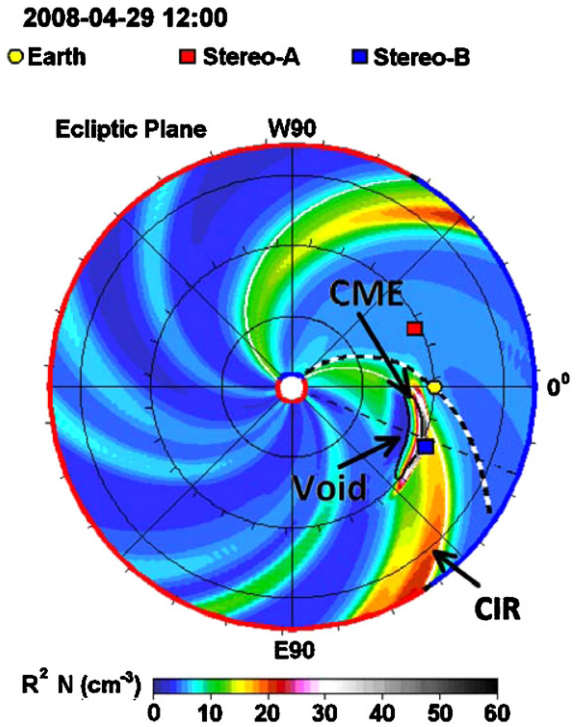

Figure 6. ENLIL density ecliptic cut viewed from the north just at the arrival time of the 2008 April 26 CME and corotating density structure at *STEREO-B* (at the date and times indicated). The Sun is at the center of each plot with the Earth a yellow dot shown to the right on its orbit. Projected locations of both *STEREO-A* and *STEREO-B* are shown ahead of and behind Earth's orbital path, respectively. In order to view structures at the same density contour level with solar distance, an r^{-2} density falloff normalized at 1 AU has been removed from the volumetric data whose scale is shown below the image. The ecliptic location of the CME is indicated by an elongated black outline (see arrow) that has just arrived at *STEREO-B* (from Odstrcil et al. 2010).

4. CONCLUSIONS

SMEI has recorded the inner-heliospheric response to the 2008 April 26 CME and a corotating dense structure that it intersects. The dense structure associated with the CME moves outward primarily north of the ecliptic; the analysis also details an ecliptic density enhancement associated with a corotating

region. This analysis yields a qualitatively similar form for the CME compared with that mapped by the *STEREO* HI-2B instrument as determined by Wood and Howard (2009) and the first of the models in Lugaz et al. (2010). There are some differences in the CME location as noted in the text compared with other analyses of the CME. We determine an excess mass of 3×10^{15} g for this event contained above a 4 N_P cm^{-3} contour level threshold, a result that compares well with the sky-plane 3.5×10^{15} g excess mass value for this CME derived from the LASCO C3 coronagraph data. We note that the CME in the SMEI analysis extends from near Earth to nearly 90° east of the Sun–Earth line and that including this uncertain multiplicative factor to the LASCO images would increase the sky plane mass derived from the LASCO coronagraph by perhaps as much as a factor of 1.5. Because of possible CME evolution from the low corona to where it is viewed in SMEI, the 4 N_P cm^{-3} contour level threshold that separates the CME from the background solar wind near 1 AU is only a rough estimate of the material encompassing the CME closer to the Sun. A different contour level threshold could incorporate more of the total CME mass of $\sim 1 \times 10^{16}$ g that we measure. Moreover, because the CME interacts with the pre-existing material of the slower-moving corotating structure, a precise mass estimate for this event is further compromised by uncertainty in locating the 3D boundary between the CME and the slower-moving corotating material. Other comparisons of SMEI-derived CME masses with LASCO CME mass measurements (some for more compact events where better comparisons can be made) are found in Jackson et al. (2006, 2008a, 2009).

The corotating region's density does not form a continuous front in the ecliptic but is broken in several places between the Sun and 1 AU. Since similar non-uniform brightnesses for such corotating structures were observed as early as the Helios observations (Jackson 1991), and more recently from *STEREO* HI-2 measurements of corotating density enhancements from HI-2 (e.g., Rouillard et al. 2010), this deserves further investigation. While we expect no significant changes to the large overall features that are three-dimensionally reconstructed, values of ± 2 N_P approach the limit of the single-element volumetric element reconstruction uncertainty in the current SMEI analyses.

The work of B.V. Jackson, A. Buffington, and M. M. Bisi was supported at the University of California, San Diego by NSF grants ATM-00852246 and ATM-0925023 and NASA grant NNX08AJ11G. More recently, M. M. Bisi acknowledges support from a rolling grant and standard grant to the Institute of Mathematics and Physics, Aberystwyth University, from the Science & Technology Facilities Council (STFC) in the UK. The work of D.F. Webb was supported at Boston College by Air Force contract FA8718-06-C-0015 and Navy grants N00173-01-1-G013 and N00173-07-1-G016. We gratefully acknowledge the *SOHO*/LASCO consortium for making the LASCO images available on the internet and determining the CME mass for the 2008 April 26 CME for use by the Coordinated Data Analysis Workshops (CDAW). This CME catalog is generated and maintained at the CDAW Data Center by NASA and The Catholic University of America in cooperation with the Naval Research Laboratory. *SOHO* is a project of international cooperation between ESA and NASA. We also gratefully acknowledge the ENLIL analysis shown in Figure 6 provided to us by D. Odstrcil from several of his recent presentations of this modeling effort including that cited. The SMEI instrument was designed and constructed by a team of scientists and engineers from the US Air Force Research Laboratory, the University of California at San Diego, Boston College, Boston University, and the University of Birmingham, UK, with additional funding from NASA.

REFERENCES

Bisi, M. M., Jackson, B. V., Hick, P. P., Buffington, A., Clover, J. M., Tokumaru, M., & Fujiki, K. 2010, ApJ, 715, L104
Brueckner, G. E., et al. 1995, Sol. Phys., 162, 357
Delaboudiniere, J.-P., et al. 1995, Sol. Phys., 162, 291
Domingo, V., Fleck, B., & Poland, A. I. 1995, Space Sci. Rev., 72, 81
Eyles, C. J., et al. 2003, Sol. Phys., 217, 319
Eyles, C. J., et al. 2009, Sol. Phys., 254, 387
Galvin, A. B., et al. 2008, Space Sci. Rev., 136, 437
Hewish, A., Scott, P. F., & Wills, D. 1964, Nature, 203, 1214
Jackson, B. V. 1991, J. Geophys. Res., 96, 11,307
Jackson, B. V., Bisi, M. M., Hick, P. P., Buffington, A., Clover, J. M., & Sun, W. 2008a, J. Geophys. Res., 113, A00A15
Jackson, B. V., Buffington, A., & Hick, P. P. 2001, in Proc. "Solar Encounter: The First Solar Orbiter Workshop," A Heliospheric Imager for Solar Orbiter, ed. B. Battrick & H. Sawaya-Lacoste (ESA SP-493; Noordwijk: ESA), 251
Jackson, B. V., Buffington, A., Hick, P. P., Wang, X., & Webb, D. 2006, J. Geophys. Res., 111, A04S91
Jackson, B. V., Hick, P. P., & Buffington, A. 2002, Proc. SPIE, 4853, 23
Jackson, B. V., Hick, P. P., Buffington, A., Bisi, M. M., & Clover, J. M. 2009, Ann. Geophys., 27, 4097
Jackson, B. V., Hick, P. P., Buffington, A., Bisi, M. M., Clover, J. M., & Tokumaru, M. 2008b, Adv. Geosci., 21, 339
Jackson, B. V., et al. 2004, Sol. Phys., 225, 177
Kaiser, M. L., Kucera, T. A., Davila, J. M., St. Cyr, O. C., Guhathakurta, M., & Christian, E. 2008, Space Sci. Rev., 136, 5
Lugaz, N., Hernandez-Charpak, J. N., Roussev, I. I., Davis, C. J., Vourlidas, A., & Davies, J. A. 2010, ApJ, 715, 493
Michałek, G., Gopalswamy, N., & Yashiro, S. 2003, ApJ, 584, 472
Mizuno, D. R., et al. 2005, J. Geophys. Res., 110, A07230
Odstrcil, D., Arge, C. N., Rasca, A., Thernisien, A., & Xie, H. 2010, Simulation of Heliospheric Disturbances Initialized by Various Fitting Techniques, NOAA Space Weather Workshop Boulder, CO, 2010 April 27–30
Rouillard, A. P., et al. 2010, J. Geophys. Res., 115, A04103
Thernisien, A., Vourlidas, A., & Howard, R. A. 2009, Sol. Phys., 256, 111
Wang, X., Hick, P. P., Jackson, B. V., & Bailey, M. 2003, Proc. SPIE, 5171, 280
Wood, B. E., & Howard, R. A. 2009, ApJ, 702, 901
Zhang, J., et al. 2007, J. Geophys. Res., 112, A10102